AIP | The Journal of Chemical Physics

# Experimental and theoretical studies of the reaction of atomic oxygen with silane

Luying Ding and Paul Marshall

Citation: The Journal of Chemical Physics **98**, 8545 (1993); doi: 10.1063/1.464513
View online: http://dx.doi.org/10.1063/1.464513
View Table of Contents: http://scitation.aip.org/content/aip/journal/jcp/98/11?ver=pdfcov
Published by the AIP Publishing

---

---

# Experimental and theoretical studies of the reaction of atomic oxygen with silane

Luying Ding and Paul Marshall
*Department of Chemistry, University of North Texas, P.O. Box 5068, Denton, Texas 76203-5068*

(Received 16 November 1992; accepted 17 February 1993)

The flash-photolysis resonance-fluorescence technique has been employed to measure the rate constant for $O+SiH_4 \rightarrow$ products from 295–565 K, and yielded $k_1 = 1.23 \times 10^{-10} \exp(-14.6 \text{ kJ mol}^{-1}/RT) \text{ cm}^3 \text{ s}^{-1}$ with an accuracy of about ±15%. The transition state for direct H-atom abstraction has been characterized at up to the Gaussian-2 *ab initio* level of theory. With small adjustments it is possible to model kinetic data for $O+SiH_4$ in terms of an abstraction channel leading to $OH+SiH_3$. This agreement does not rule out minor participation by addition or insertion channels, but there is no theoretical evidence for bound triplet intermediates in the potential energy surface. A transition state theory analysis suggests that $k_1$ at 1000 K is 16 times larger than previously thought.

## I. INTRODUCTION

Knowledge of the rate constant $k_1$ for the reaction of ground state atomic oxygen, $O(2p)^3P_J$, with $SiH_4$ at elevated temperatures

$$O+SiH_4 \rightarrow \text{products} \tag{1}$$

is needed to model the chemistry of $SiH_4$ flames and explosions[1–7] and silicon oxide chemical vapor deposition (CVD) from mixtures of $SiH_4$ with $O_2$ or $N_2O$.[8–14] There are significant deficiencies and discrepancies in the existing data for reaction (1), especially at high temperatures, and part of the impetus for our work is to obtain a good description of the temperature dependence of $k_1$. The first part of the present work describes experimental measurements of $k_1$ at up to 565 K carried out with the flash-photolysis resonance-fluorescence (FP-RF) technique, using an apparatus which has already been shown to give $k_1$ results at room temperature[15] in accord with other techniques.[16–18]

There have been two previous kinetic studies carried out above room temperature, one by Atkinson and Pitts who employed flash-photolysis with O/NO chemiluminescence detection of O atoms (FP-CL) and obtained $k_1 = 6.8 \times 10^{-12} \exp(-6.6 \text{ kJ mol}^{-1}/RT) \text{ cm}^3 \text{ s}^{-1}$ over 297–438 K,[16] while discharge-flow experiments by Mkryan *et al.* with ESR detection of O (DF-ESR) yielded $k_1 = 2.7 \times 10^{-11} \exp(-11.3 \text{ kJ mol}^{-1}/RT) \text{ cm}^3 \text{ s}^{-1}$ over 280–549 K.[17] The first of these Arrhenius expressions is recommended for use up to 1000 K,[19] but the alternative expressions yield $k_1$ values that differ by a factor of 5 if extrapolated to 1000 K. The pre-exponential $A$ factors, especially the former, seem unusually small when compared to those found for O+hydrocarbon reactions. For instance, $A \approx 1.0 \times 10^{-10} \text{ cm}^3 \text{ s}^{-1}$ over the range 400–700 K for the reaction of atomic oxygen with the $SiH_4$ analog, $CH_4$.[19] Another area of disagreement concerns the products of reaction (1). Chemiluminescence and laser-induced fluorescence studies of OH by Agrawalla and Setser[20] and Park *et al.*,[21] as well as a mass-spectrometric product study by Horie *et al.*,[18] suggest that the dominant channel is

$$O+SiH_4 \rightarrow SiH_3+OH. \tag{1a}$$

Such a reaction is important in combustion because it increases the number of radicals, while $SiH_3$ is thought to be a major species in CVD.[22] However, Withnall and Andrews[23] observed formation of (singlet) $SiH_3OH$ in matrix isolation experiments and proposed that reaction (1) proceeds via an addition/insertion mechanism, which implies a bound triplet $OSiH_4$ intermediate and would be nonadiabatic with respect to spin. Herron[19] instead suggested that $SiH_3OH$ was formed from recombination of the products of reaction (1a) in the matrix.

There have been semiempirical theoretical studies of silane reactivity, but Horie *et al.* noted that the BEBO method "fails completely" for the reactions of O with silanes.[18] The second part of this work describes the first *ab initio* study of the mechanism of reaction (1), the prototypical O+silane reaction. This was made to test whether the abstraction channel (1a) can account for the observed kinetics, and to search for possible triplet $OSiH_4$ intermediates. The theoretical work also checks the magnitude of the pre-exponential $A$ factor, and permits reliable extrapolation of $k_1$ beyond the experimental temperature range.

## II. EXPERIMENTAL MEASUREMENTS

### A. Technique

Details of the variable-temperature reactor,[24] the general FP-RF method,[25] and modifications for the study of atomic O[15] have been given elsewhere. A mixture of $SO_2$ and $SiH_4$ diluted in a large excess of Ar bath gas flowed through the reactor which operated pseudostatically. The bath gas maintained isothermal conditions and slowed diffusion of atomic oxygen to the reactor walls, and the temperature was measured with a thermocouple corrected for radiation errors.[26] O atoms were produced by flash-photolysis of $SO_2$, in an initial concentration $[O]_0 \ll [SiH_4]$, so that

$$\frac{-d[O]}{dt} = k_1[SiH_4][O] + k_{\text{diff}}[O] = k_{\text{ps1}}[O], \tag{2}$$

TABLE I. Summary of rate constant measurements for $O+SiH_4$.

| $T$ (K) | $P$ (mbar) | $\tau_{res}$ (s) | $F$ (J) | $[SO_2]$ $10^{15}$ ($cm^{-3}$) | $[SiH_4]_{max}$ $10^{14}$ ($cm^{-3}$) | $k_1 \pm \sigma_{k1}$ $10^{-13}$ ($cm^3$ $s^{-1}$) |
|---|---|---|---|---|---|---|
| 295 | | | | | | 3.0 ±0.2[a,b] |
| 333 | 52 | 2.4 | 4.05 | 4.41 | 1.55 | 6.08±0.16 |
| 333 | 101 | 1.5 | 4.05 | 3.39 | 0.99 | 5.98±0.25 |
| 333 | 103 | 2.9 | 4.05 | 6.71 | 1.97 | 7.19±0.20 |
| 333 | 200 | 3.0 | 4.05 | 6.70 | 1.96 | 6.90±0.17 |
| 333 | | | | | | 6.5 ±0.3[b] |
| 378 | 101 | 3.0 | 5.00 | 5.98 | 1.95 | 13.0 ±0.3 |
| 378 | 101 | 3.0 | 2.45 | 5.98 | 1.95 | 10.0 ±0.9 |
| 378 | 205 | 3.0 | 5.00 | 6.12 | 1.99 | 12.8 ±0.3 |
| 378 | 205 | 3.0 | 2.45 | 6.12 | 1.99 | 14.2 ±0.3 |
| 378 | | | | | | 12.5 ±0.9[b] |
| 466 | 133 | 1.0 | 5.00 | 2.70 | 1.01 | 27.5 ±1.1 |
| 466 | 133 | 1.0 | 2.45 | 2.70 | 1.01 | 27.1 ±1.2 |
| 466 | 133 | 1.0 | 5.00 | 4.77 | 1.01 | 25.7 ±0.8 |
| 466 | 133 | 1.0 | 2.45 | 4.77 | 1.01 | 27.8 ±1.4 |
| 466 | 133 | 3.0 | 5.00 | 4.87 | 1.48 | 25.7 ±1.4 |
| 466 | 133 | 3.0 | 2.45 | 4.87 | 1.48 | 20.5 ±2.9 |
| 466 | 135 | 1.0 | 5.00 | 2.31 | 0.35 | 28.5 ±0.6 |
| 466 | 135 | 1.0 | 2.45 | 2.31 | 0.35 | 27.7 ±0.7 |
| 466 | 135 | 3.0 | 5.00 | 3.87 | 0.69 | 24.4 ±0.5 |
| 466 | 135 | 3.0 | 2.45 | 3.87 | 0.69 | 27.0 ±1.8 |
| 466 | | | | | | 26.2 ±0.7[b] |
| 563 | 268 | 1.5 | 4.05 | 3.09 | 0.35 | 60.1 ±1.4 |
| 564 | 272 | 3.0 | 4.05 | 2.03 | 0.35 | 45.1 ±1.3 |
| 565 | 67 | 0.5 | 4.05 | 2.50 | 0.23 | 57.0 ±1.4 |
| 566 | 69 | 1.0 | 4.05 | 3.88 | 0.35 | 68.4 ±1.7 |
| 566 | 68 | 3.0 | 4.05 | 3.74 | 0.33 | 53.7 ±1.3 |
| 565 | | | | | | 56.9 ±3.8[b] |

[a] See Ref. 15.
[b] Mean and s.d. of mean.

where $k_{ps1}$ is the pseudo-first-order rate constant and $k_{diff}$ accounts for diffusional loss of O from the reaction zone and recombination of O with $SO_2$. $[O]_0$ was varied by changing $[SO_2]$ or the energy of the flash-lamp discharge, $F$. A microwave-powered discharge lamp excited resonance fluorescence at 130 nm, $O(3s)^3S \rightarrow O(2p)^3P_J$,[27] which was monitored by a solar-blind photomultiplier tube operated with pulse-counting and signal-averaging. $k_{ps1}$ values were obtained by nonlinear least-squares fits to the exponential decays of fluorescence intensity,[28] and $k_1$ values as the slopes of weighted linear plots[29] of typically 5 or 6 $k_{ps1}$ values as a function of $[SiH_4]$ from 0 to $[SiH_4]_{max}$.

### B. Results

Twenty-three $k_1$ determinations at four temperatures from 333 to 565 K are summarized in Table I, where the quoted uncertainties represent precision only. $P$ was varied by a factor of 5, the average gas residence time within the reactor before photolysis, $\tau_{res}$, by a factor of 6, $F$ by a factor of 2 and $[SO_2]$ by a factor of 3. There was no consistent variation of $k_1$ with $\tau_{res}$, which demonstrates that thermal decomposition of $SiH_4$ was unimportant, nor a significant variation with the product $F[SO_2]$, i.e., $[O]_0$, which is consistent with attainment of pseudo-first-order conditions and successful isolation of reaction (1) from secondary chemistry. We averaged the $k_1$ determinations at each temperature, weighting them equally, and derived the standard deviation of the mean. This standard deviation reflects the reproducibility of the individual $k_1$ measurements. The value of $k_1$ obtained from 19 measurements at 295 K made earlier in the same apparatus[15] is also shown in Table I.

The five averaged $k_1$ results are plotted in Fig. 1 in Arrhenius form. The weighted fit to $A \exp(-E_a/RT)$, which takes into account both the uncertainty in $T$, about 2%, and the averaged $k_1$ values, yields

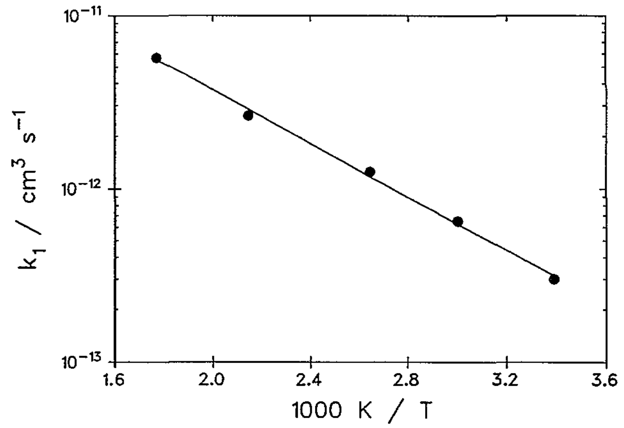

FIG. 1. Arrhenius plot summarizing 42 determinations of $k_1$ for $O+SiH_4$ at five temperatures.

TABLE II. HF/6-31G* and MP2/6-31G* geometries.[a]

| Species | Symmetry | HF/6–31G* | | MP2/6–31G* | |
|---|---|---|---|---|---|
| $SiH_4$ | $T_d$ | $r_{\text{Si-H}}$ 1.475, | ∠HSiH 109.47 | $r_{\text{Si-H}}$ 1.483, | ∠HSiH 109.47 |
| $OSiH_4^\ddagger$ | $C_s$ | $r_{\text{O-Ha}}$ 1.205, | $r_{\text{Si-Ha}}$ 1.747, | $r_{\text{O-Hb}}$ 1.310, | $r_{\text{Si-Ha}}$ 1.627, |
| | | $r_{\text{Si-Hb}}$ 1.473, | $r_{\text{Si-Hc}}$ 1.473, | $r_{\text{Si-Hb}}$ 1.481, | $r_{\text{Si-Hc}}$ 1.481, |
| | | $\angle OH_aSi$ 178.52, | $\angle H_aSiH_b$ 108.54, | $\angle OH_aSi$ 174.86, | $\angle H_aSiH_b$ 108.63, |
| | | $\angle H_aSiH_c$ 107.62, | $\angle H_bSiH_c$ 111.03 | $\angle H_aSiH_c$ 107.48, | $\angle H_bSiH_c$ 111.14 |
| OH | $C_{\infty v}$ | $r_{\text{O-H}}$ 0.959 | | $r_{\text{O-H}}$ 0.979 | |
| $SiH_3$ | $C_{3v}$ | $r_{\text{Si-H}}$ 1.476, | ∠HSiH 110.88 | $r_{\text{Si-H}}$ 1.483, | ∠HSiH 111.25 |

[a] Bond lengths in $10^{-10}$ m, and angles in degrees.

$$k_1=(1.23\pm0.18)\times10^{-10} \times\exp(-14.6\pm0.5\ \text{kJ mol}^{-1}/RT)\text{cm}^3\ s^{-1} \quad (3)$$

for $295\ \text{K} \leqslant T \leqslant 565$ K. The uncertainties in $A$ and $E_a$ represent $\pm 1\sigma$. The uncertainty in $k_1$ is smaller, because errors in $A$ and $E_a$ are coupled, and consideration of the covariance[30] yields $1\sigma$ for $k_1$ that varies from 3.5% in the middle of the $1/T$ range up to about 6% at the ends. Comparison between different techniques at room temperature suggests that any systematic errors are small.[15] Allowance of ±5% for possible but unrecognized systematic errors yields a 95% accuracy for $k_1$ of about ±15%.

## III. THEORETICAL ANALYSIS

*Ab initio* calculations were carried out with the GAUSSIAN90 program[31] on a VAX 6310 and a Solbourne 5E/902 computer, using theoretical methods outlined by Hehre *et al.*[32] The geometries of the species of reaction (1a) and the corresponding transition state (TS), $SiH_4O^\ddagger$, were optimized with the 6–31G* atomic basis set at the self-consistent field or Hartree–Fock (HF) and MP2 levels of theory. The latter level makes a partial correction for electron correlation. Spin-unrestricted UHF wave functions were employed for open-shell species, and spin-restricted RHF wave functions for $SiH_4$. Next, vibrational frequencies were calculated at each stationary point on the potential energy surface (PES), to verify them as true minima, with all real frequencies, or the TS, with a single imaginary frequency. The HF and MP2 frequency results were scaled by factors of 0.893 and 0.95, respectively, before calculation of the zero-point vibrational energies (ZPE) of each species. The wavefunctions at the stationary points were verified to be HF stable.[33] The Gaussian-2 (G2) methodology of Pople and co-workers, a series of additive corrections to the MP4/6–311G**//MP2/6–31G* energy, was then applied to obtain *approximate* QCISD(T)/6–311+G**(3*df*,2*p*)//MP2/6–31G* energies.[34–36] Combination of these electronic energies with the ZPE allows estimation of $\Delta H_0$, the enthalpy change for reaction (1a) at 0 K, and $E_0^\ddagger$, the enthalpy of the TS relative to $O+SiH_4$ at 0 K. The G2 method calls for use of the HF/6–31G* ZPE. We have also employed the MP2/6–31G* ZPE and denote the results as G2*. The G2 method makes no allowance for errors arising from spin contamination: here we define a spin-projected P-G2 energy as the G2 value plus a correction equal to the difference between the PMP4/6–311G** and MP4/6–311G** energies, where spin contamination has been projected out of the PMP4 energy using the algorithm of Schlegel.[37] An alternative approach to estimating $E_0^\ddagger$ was also applied, the MP-SAC4 method of Gordon and Truhlar.[38,39] In this approach, the MP4 correlation energy of the TS is scaled by a factor derived from comparison of MP4 and experimental dissociation energies $D_e$ for $SiH_3$–H and O–H.

Simple transition state theory[40,41] (TST) was employed to analyze the kinetics of channel (1a)

$$k_{\text{TST}}=l^\ddagger \frac{k_BT}{h}\frac{Q^\ddagger}{Q_OQ_{SiH_4}}\exp\left(-\frac{E_0^\ddagger}{RT}\right), \quad (4)$$

where $l^\ddagger$ is the reaction path degeneracy, and the $Q$'s are the partition functions. Each $Q$ is estimated from the MP2/6–31G* data with the usual assumption of the separability of vibrational and rotational motions.[42] As argued by Cohen and Westberg, only six of the nine states of $O(^3P_J)$ correlate with the products; the experimental electronic partition function $Q_{\text{el}}$ for O is $5+3\exp(-228\ \text{K}/T)+\exp(-326\ \text{K}/T)$, $Q_{\text{el}}$ for $SiH_4$ is 1, and a value of six was assumed for $Q_{\text{el}}$ for the TS.[41] Rotational symmetry factors were set equal to 1, and symmetry was taken into account via $l^\ddagger=4$.

## IV. DISCUSSION

### A. Comparison between measured $k_1$ values

Our data at 295 K have already been shown to be in accord with those from most other experimental techniques at room temperature.[15–18] Figure 3 is an Arrhenius plot of Eq. (3) together with the best-fit rate constant expressions from the FP-CL work of Atkinson and Pitts[16] and the DF-ESR work of Mkryan *et al.*[17] It may be seen that while there is accord to within about a factor of 1.5 between the three expressions at $T \leqslant 400$ K, above 400 K there are significant differences, with the present work lying higher than the earlier results. This reflects the different Arrhenius parameters measured here.

### B. Comparison between theory and experiment for O, $SiH_4$, $SiH_3$, and OH

The *ab initio* geometries for minima in the PES shown in Table II and Fig. 2 are, of course, identical with previous

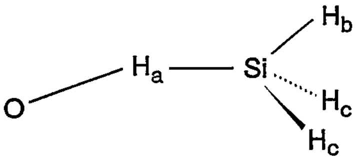

FIG. 2. Structure of the transition state for $O+SiH_4 \rightarrow OH+SiH_3$.

equivalent calculations where they exist.[32,43] Typically MP2 theory leads to longer bonds than HF theory,[32] and this can be seen in Table II. For OH and $SiH_4$ the MP2 bond lengths are closer to the experimental values[44] and we therefore employ results from MP2 theory in the kinetic calculations below.

Vibrational frequencies at stationary points in the $O+SiH_4$ PES are summarized in Table III. For $SiH_4$ the mean absolute error is 34 $cm^{-1}$ at the HF level and 18 $cm^{-1}$ at the MP2 level, relative to the measured frequencies.[44] For $SiH_3$ the lowest mode has been measured to be $\approx 724$ $cm^{-1}$,[45] 57 and 41 $cm^{-1}$ below the HF and MP2 estimates, respectively. For OH the errors at the scaled HF and MP2 levels are 0 and 16 $cm^{-1}$, respectively.[46] The similarity of the HF and MP2 frequencies means that the corresponding ZPE are essentially identical, and that there is a negligible difference between the G2 and G2* energies.

*Ab initio* energies for O, $SiH_4$, $SiH_3$, and OH have been listed elsewhere;[34–36] new results for $SiH_4O^\ddagger$ are shown in Table IV. The theoretical $\Delta H_0$ for reaction (1a) listed in Table V can be tested against the experimental value derived from the measured $\Delta H_{f,298}(SiH_3)$[47] together with $H_{298}-H_0(SiH_3)$ calculated by Hudgens[48] and $\Delta H_{f,0}$ for O, $SiH_4$, and OH.[44] As the size of the basis set is increased there is a monotonic improvement in $\Delta H_0$. Only the highest and computationally most demanding levels of theory, G1, G2, and MP-SAC4/6–311+G**//MP2/6–31G*, give results within 10 kJ $mol^{-1}$ of experiment, probably because of the large changes in electron correlation for the O atom in the course of reaction. The small degree of spin-contamination in the UHF/6–311G** wave functions of the products OH and $SiH_3$ ($\langle S^2\rangle=0.755$ and 0.756, respectively, versus the ideal value of 0.75 for doublets) is slightly greater than for the reactants ($\langle S^2\rangle=2.005$ for O vs the ideal value of 2 for a triplet), so that at the P-G2 level of theory $\Delta H_0$ is slightly more negative and yields excellent accord with experiment.

TABLE IV. Components of the G2 energy for the $SiH_4O^\ddagger$ transition state.[a]

| Calculation | Energy |
|---|---|
| Zero-point energy | 0.026 07[b] |
| MP4/6–311G** | −366.314 48 |
| PMP4/6–311G** | −366.317 49 |
| MP4/6–311+G** | −366.321 24 |
| MP4/6–311G**(2*df*) | −366.370 30 |
| QCISD(T)/6–311G** | −366.320 10 |
| MP2/6–311G** | −366.268 88 |
| MP2/6–311+G** | −366.274 94 |
| MP2/6–311G**(2*df*) | −366.318 25 |
| MP2/6–311+G(3*df*,2*p*) | −366.331 74 |

[a] At the MP2/6–31G* optimized geometry. Electronic energies are quoted in atomic units: 1 hartree$\approx$2625 kJ $mol^{-1}$.

[b] Based on HF/6-31G* frequencies at the HF/6-31G* optimized geometry, scaled by 0.893.

## C. Properties of the transition state

The MP2 geometry of the TS, by comparison with the HF data, suggests that inclusion of electron correlation yields a TS earlier along the reaction coordinate, with a longer O–H partial bond and a shorter Si–H partial bond, although the vibrational frequencies at both levels of theory, especially the lower modes that contribute most strongly to $Q^\ddagger$, are very similar. The differences in geometry make only a small change in the rotational partition function. As seen from the discussion of $\Delta H_0$ in the preceding section, values of $E_0^\ddagger$ from levels of theory lower than G1, G2, and MP-SAC4/6–311+G**//MP2/6–31G* are unreliable, and the best purely *ab initio* estimate is $E_0^\ddagger \approx 11$ kJ $mol^{-1}$ at the P-G2 level. This value is close to the measured $E_a$, although it should be noted that the G2 method has *not* been parameterized nor recommended for transition states,[34–36] and that $E_a \neq E_0^\ddagger$.

A more accurate assessment of $E_0^\ddagger$ is obtained by fitting Eq. (4) to our measured $k_1$, on the assumption that $k_1 \approx k_{1a}$. Agreement between Eqs. (3) and (4) with a root-mean-square deviation of about 11% is obtained with $E_0^\ddagger = 11.8$ kJ $mol^{-1}$. This estimate is somewhat dependent on the kind of TST employed, so a reasonable conservative estimate of the uncertainty is around 3 kJ $mol^{-1}$. The error in the P-G2 barrier height is only about 0.5 kJ $mol^{-1}$, which is probably fortuitously small, but certainly lies within the target accuracy for the G2 method.

TABLE III. HF/6-31G* and MP2/6-31G* frequencies.[a]

| Species | HF/6–31G* | MP2/6–31G* |
|---|---|---|
| $SiH_4$ | 907 (3), 939 (2), 2131 (3), 2138 | 909 (3), 955 (2), 2207, 2220 (3) |
| $SiH_4O^\ddagger$ | 2355*i*, 157, 223, 349, 794, 827,<br>850, 908, 910, 2134, 2143, 2147 | 1985*i*, 149, 238, 440, 820, 832,<br>867, 920, 927, 2211, 2235, 2238 |
| OH | 3569 | 3553 |
| $SiH_3$ | 781, 906 (2), 2111, 2128 (2) | 765, 922 (2), 2186, 2222 (2) |

[a] Vibrational frequencies in $cm^{-1}$, scaled by 0.893 at the HF/6–31G* level and 0.95 at the MP2/6–31G* level. Degeneracies are shown in parentheses.

TABLE V. Enthalpies of the transition state and products relative to reactants at 0 K, $E_0^\ddagger$ and $\Delta H_0$, for $O+SiH_4 \rightarrow SiH_4O^+ \rightarrow OH+SiH_3$.

| Calculation | $E_0^\ddagger$ (kJ mol$^{-1}$) | $\Delta H_0$ (kJ mol$^{-1}$) |
|---|---|---|
| HF/6–31G*[a] | 119.0 | 50.7 |
| MP2/6–31G*[b] | 50.7 | −26.6 |
| MP4/6–31G*[b] | 50.9 | −16.4 |
| MP-SAC4/6-31G* | 5.6 | −70.8 |
| MP4/6–311G**[b] | 43.2 | −21.1 |
| PMP4/6–311G**[b] | 37.1 | −22.4 |
| MP-SAC4/6-311G**[b] | 31.8 | −32.6 |
| MP4/6–311+G**[b] | 36.4 | −30.0 |
| MP-SAC4/6-311+G** | 25.9 | −40.3 |
| G1[c] | 18.4 | −38.1 |
| G2[c] | 17.4 | −42.9 |
| G2*[b] | 17.7 | −43.6 |
| P-G2[c] | 11.3 | −44.9 |
| Expt. (see the text) | 11.8±3.0 | −46.4±2.0 |

[a] At the HF/6–31G* optimized geometry, including scaled zero-point energy (ZPE) at the HF/6–31G* level.

[b] At the MP2/6–31G* optimized geometry, including scaled ZPE at the MP2/6–31G* level.

[c] At the MP2/6–31G* optimized geometry, including scaled ZPE at the HF/6–31G* level.

## D. Kinetic implications

Use of $E_0^\ddagger=11.8$ kJ mol$^{-1}$ leads to the following TST expression for 295 K $\leqslant T \leqslant$ 2000 K,

$$k_{1a}=5.1\times10^{-17}(T/\mathrm{K})^{2.15}\exp(-1062\ \mathrm{K}/T)\mathrm{cm}^3\,\mathrm{s}^{-1}, \tag{5}$$

which fits the measured $k_1$ to within the experimental uncertainty. This expression is plotted on Fig. 3 and the accord with Eq. (4) provides theoretical support to the $A$ factor measured here. This $A$ factor lies within a factor of 1.4 of that measured for $O+CH_4$ (Ref. 19) and those measured for $Cl+SiH_4$ and $Br+SiH_4$.[25] Equation (5) also provides a reasonable extrapolation of $k_1$ beyond the measured range. The $k_1$ values implied at higher temperatures are significantly greater than recommended earlier:[19] for example, at 1000 K we suggest $k_1 \approx 5.0\times10^{-11}$ cm$^3$ s$^{-1}$ which is about 16 times greater than the recommendation. Thus reaction (1) may be more important in combustion and CVD chemistry than previously thought.

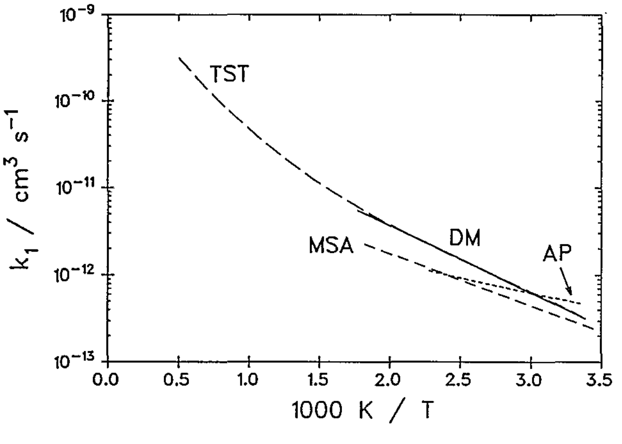

FIG. 3. Comparison of fits to $k_1$: present measurements (DM); Atkinson and Pitts, Ref. 16 (AP); Mkryan *et al.*, Ref. 17 (MSA); transition state theory (TST).

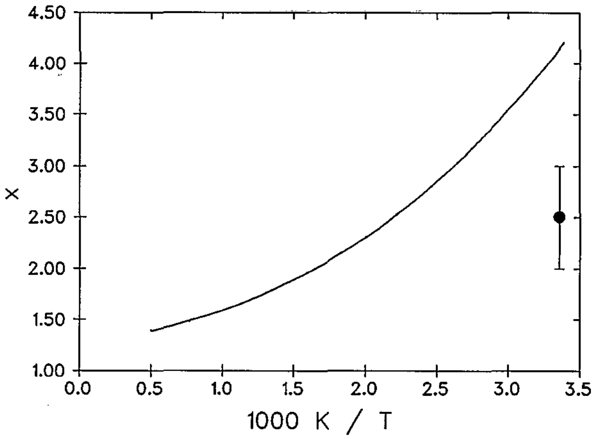

FIG. 4. Comparison of computed kinetic isotope effect $x=k_1(O+SiH_4)/k_1(O+SiD_4)$ (—) with the measurement of Horie *et al.*, Ref. 18 (●).

No explicit allowance for quantum mechanical tunneling has been made, because with the small $E_0^\ddagger$ of around 10 kJ mol$^{-1}$ classical passage of reactants over the barrier dominates any tunneling contribution.[49] A sensitive test of the present application of simple TST is whether the kinetic isotope effect, quantified here as $x=k_{1a}(O+SiH_4)/k_{1a}(O+SiD_4)$, is correctly predicted. New moments of inertia, frequencies and ZPE for deuterated $SiH_4$ and $SiH_4O^\ddagger$ and unchanged electronic energies were employed with Eq. (3). The results over the range 295–2000 $K$ may be approximately summarized as

$$x \approx 0.30(T/\mathrm{K})^{0.17}\exp(493\ \mathrm{K}/T). \tag{6}$$

At the high temperature limit $x$ approaches $\sqrt{2}$ as all the terms in the ratio of TST expressions cancel except for the ratios of the rotational partition functions. At room temperature $x \approx 4$ and is dominated by the higher effective barrier $E_0^\ddagger$ in the deuterated case. This higher barrier arises from a smaller loss of ZPE going from the reactants to the TS for the deuterated species. Figure 4 shows a comparison of Eq. (6) with the experimental determination by Horie *et al.* at room temperature,[18] where we have estimated approximate error limits for $x$ of ±20%. That value falls somewhat below the theoretical line. One possible interpretation is that the high frequencies in the TS are overestimated: if the three highest were reduced by about 200 cm$^{-1}$ each then the experimental and theoretical $x$ would agree while $Q^\ddagger$ (and thus $k_1$) would be largely unaffected. Any role for tunneling would increase $x$ and increase the divergence from experiment. Thus it is possible to rationalize *all* the kinetic data, with only minor modifications to the *ab initio* information, in terms of a single direct abstraction channel (1a) that leads to OH formation.

## E. Addition or insertion channels

A search of the triplet $O+SiH_4$ PES was carried out at the correlated MP2/6-31G* level for possible adducts or stable insertion species. A $C_{3v}$ van der Waals adduct between O and $SiH_4$ was found, with the O atom 3.6 Å from the Si, opposite from an Si–H bond, and with all real vibrational frequencies. G2* theory suggests this adduct is about 8 kJ $mol^{-1}$ *endothermic* with respect to $O+SiH_4$, so this adduct is not expected to influence the kinetics significantly. No other bound pentacoordinated $^3OSiH_4$ structures, or insertion products such as $^3SiH_3OH$, were located, so that at present *ab initio* theory supports abstraction as the main reaction mechanism in accord with the recommendation of Herron[19] and the discussion of Horie *et al.*[18] Insertion with a simultaneous spin-flip is possible, but would proceed with a reduced probability and is unlikely to make a major contribution to $O(^3P)$ consumption.

## V. CONCLUSIONS

The rate constant $k_1$ for $O+SiH_4 \rightarrow$ products has been determined over the temperature range 295–565 K. Kinetic data for this reaction have been successfully modeled in terms of an abstraction mechanism to form $OH+SiH_3$, using *ab initio* information to characterize the transition state. Tunneling appears to be unimportant, and the G2 estimate of the energy barrier lies within about 6 kJ $mol^{-1}$ of the experimental value. Correction for spin-contamination yields essentially exact accord. Transition state theory permits extrapolation of $k_1$ to higher temperatures, and indicates that reaction (1) is faster than previously thought. No theoretical evidence was found for addition or insertion channels proceeding via triplet intermediates.

## ACKNOWLEDGMENTS

This work was supported by Texas Instruments, Inc., the Robert A. Welch Foundation (Grant No. B-1174), and the U.N.T. Organized Research Fund.

[1] J. R. Hartman, J. Famil-Ghiriha, M. A. Ring, and H. E. O'Neal, Combust. Flame. **68**, 43 (1987).
[2] C. J. Jachimowski and A. G. McLain, NASA Tech. Paper **2129** (1983).
[3] A. G. McLain, C. J. Jachimowski, and R. C. Rogers, NASA Tech. Paper **2415** (1985).
[4] S. Koda and O. Fujiwara, Combust. Flame. **73**, 187 (1988).
[5] K. Tokuhashi, S. Horiguchi, Y. Urano, M. Iwasaka, H. Ohtani, and S. Kondo, Combust. Flame. **82**, 40 (1990).
[6] V. V. Azatyan and R. G. Aivazyan, Kinet. Catal. **32**, 1149 (1991).
[7] S. Fukutani, Y. Uodome, N. Kunioshi, and H. Jinno, Bull. Chem. Soc. Jpn. **64**, 2328 (1991).
[8] C. Cobianu and C. Pavelescu, Thin Solid Films **102**, 361 (1983).
[9] S. Vepřek, Thin Solid Films **130**, 135 (1985).
[10] S. Yokoyama, D. W. Dong, D. J. DiMaria, and S. K. Lai, J. Appl. Phys. **54**, 7058 (1983).
[11] J. M. Jasinski, B. S. Meyerson, and B. A. Scott, Ann. Rev. Phys. Chem. **38**, 109 (1987).
[12] J. D. Chapple-Sokol, C. J. Giunta, and R. G. Gordon, J. Electrochem. Soc. **136**, 2993 (1989).
[13] C. J. Giunta, J. D. Chapple-Sokol, and R. G. Gordon, J. Electrochem. Soc. **137**, 3237 (1990).
[14] M. Liehr and S. A. Cohen, Appl. Phys. Lett. **60**, 198 (1992).
[15] C. A. Taylor, L. Ding, and P. Marshall, Int. J. Chem. Kinet. **25**, 183 (1993).
[16] R. Atkinson and J. N. Pitts, Jr., Int. J. Chem. Kinet. **10**, 1151 (1978).
[17] T. G. Mkryan, E. N. Sarkisyan, and S. A. Arutyunyan, Arm. Khim. Zh. **34**, 3 (1981); S. A. Kharutunyan, T. G. Mkryan, E. N. Sarkisyan, Oxid. Commun. **7**, 49 (1984).
[18] O. Horie, R. Taege, B. Reimann, N. L. Arthur, and P. Potzinger, J. Phys. Chem. **95**, 4393 (1991).
[19] J. T. Herron, J. Phys. Chem. Ref. Data **17**, 967 (1988).
[20] B. S. Agrawalla and D. W. Setser, J. Chem. Phys. **86**, 5421 (1987).
[21] C. R. Park, G. D. White, and J. R. Wiesenfeld, J. Phys. Chem. **92**, 152 (1988).
[22] K. J. Ryan and I. C. Plumb, CRC Crit. Rev. Solid State Mater. Sci. **15**, 153 (1988).
[23] R. Withnall and L. Andrews, J. Phys. Chem. **89**, 3251 (1985).
[24] Y. Shi and P. Marshall, J. Phys. Chem. **95**, 1654 (1991).
[25] L. Ding and P. Marshall, J. Phys. Chem. **96**, 2197 (1992).
[26] L. Ding and P. Marshall, J. Chem. Soc. Faraday Trans. **89**, 419 (1993).
[27] H. Okabe, *Photochemistry of Small Molecules* (Wiley, New York, 1978).
[28] P. Marshall, Comput. Chem. **11**, 219 (1987); **13**, 103 (1989).
[29] J. A. Irvin and T. I. Quickenden, J. Chem. Educ. **60**, 711 (1983).
[30] K. Héberger, S. Kemény, and T. Vidóczy, Int. J. Chem. Kinet. **19**, 171 (1987).
[31] M. J. Frisch, M. Head-Gordon, G. W. Trucks, J. B. Foresman, H. B. Schlegel, K. Raghavachari, M. A. Robb, J. S. Binkley, C. Gonzalez, D. J. DeFrees, D. J. Fox, R. A. Whiteside, R. Seeger, C. F. Melius, J. Baker, R. L. Martin, L. R. Kahn, J. J. P. Stewart, S. Topiol, and J. A. Pople, GAUSSIAN90 (Gaussian, Pittsburgh, 1990).
[32] W. J. Hehre, L. Radom, P. v. R. Schleyer, and J. A. Pople, *Ab Initio Molecular Orbital Theory* (Wiley, New York, 1986).
[33] R. Seeger and J. A. Pople, J. Chem. Phys. **66**, 3045 (1977).
[34] J. A. Pople, M. Head-Gordon, D. J. Fox, K. Raghavachari, and L. A. Curtiss, J. Chem. Phys. **90**, 5622 (1989).
[35] L. A. Curtiss, C. Jones, G. W. Trucks, K. Raghavachari, and J. A. Pople, J. Chem. Phys. **93**, 2537 (1990).
[36] L. A. Curtiss, K. Raghavachari, G. W. Trucks, and J. A. Pople, J. Chem. Phys. **94**, 7221 (1991).
[37] H. B. Schlegel, J. Chem. Phys. **84**, 4530 (1986).
[38] M. S. Gordon and D. G. Truhlar, J. Am. Chem. Soc. **108**, 5412 (1986).
[39] T. N. Truong, D. G. Truhlar, K. K. Baldridge, M. S. Gordon, and R. Steckler, J. Chem. Phys. **90**, 7137 (1989).
[40] K. J. Laidler, *Theories of Chemical Reaction Rates* (McGraw-Hill, New York, 1969), Chaps. 4 and 5.
[41] N. Cohen and K. R. Westberg, Int. J. Chem. Kinet. **18**, 99 (1986).
[42] G. N. Lewis and M. Randall, *Thermodynamics*, 2nd ed., revised by K. S. Pitzer and L. Brewer (McGraw-Hill, New York, 1961), Chap. 27.
[43] A. Tachibana, Y. Kurosaki, K. Yamaguchi, and T. Yamabe, J. Phys. Chem. **95**, 6849 (1991).
[44] M. W. Chase, Jr., C. A. Davies, J. R. Downey, Jr., D. J. Frurip, R. A. McDonald, and A. N. Syverud, JANAF Thermochemical Tables, 3rd ed. [J. Phys. Chem. Ref. Data **14** Suppl. No. 1. (1985)].
[45] M. E. Jacox, J. Phys. Chem. Ref. Data **17**, 269 (1988).
[46] Compared with $\nu$ for $v=0 \rightarrow v=1$ of OH, derived from data in Ref. 44.
[47] J. A. Seetula, Y. Feng, D. Gutman, P. W. Seakins, and M. J. Pilling, J. Phys. Chem. **95**, 1658 (1991).
[48] J. W. Hudgens (personal communication, 1992).
[49] Any small tunneling contributions are implicitly taken into account by a slight lowering of the effective $E_0^\ddagger$ as discussed in Ref. 41.